Synthesis and characterization of tin oxide/carbon aerogel composite electrodes for electrochemical supercapacitors

Sung-Woo Hwang, Sang-Hoon Hyun *

School of Advanced Materials Science and Engineering, Yonsei University, 134 Shinchon-dong, Seodaemun-gu, Seoul 120-749, South Korea

Abstract

Two types of carbon aerogel-based functional electrodes for supercapacitor applications are developed. To improve the electrochemical performance of the electrodes, carbon aerogels are doped with pseudocapacitive tin oxide either by impregnating tin oxide sol into resorcinol–formaldehyde (RF) wet gels (Method I), or by impregnating tin tetrachloride solution into carbon aerogel electrodes (Method II). The electrodes are heat-treated to 450 °C in air to activate the electrode surface and complete the oxidation of tin-precursors in the network structure of the aerogel. The effects of different impregnation methods on the physical/electrochemical properties of the composite electrodes are investigated. Microstructural and compositional variations of the electrodes with tin oxide doping are also examined by scanning electron microscopy and energy dispersive X-ray analysis. The tin oxide/carbon aerogel composite electrodes synthesized by both methods have similar specific capacitances (66–70 F g^{-1}). Composite electrodes synthesized via Method II showed better cyclic stability compared with electrodes synthesized via Method I.
© 2007 Elsevier B.V. All rights reserved.

Keywords: Supercapacitor; Electrical double-layer capacitor; Pseudocapacitor; Carbon aerogel; Tin oxide; Ambient drying

1. Introduction

New electrochemical energy-storage devices, such as supercapacitors have received significant attention recently due to their high specific capacitance and long cycle-life [1,2]. In the past few decades, numerous research articles [1–12] have outlined the development of novel candidate materials for supercapacitor applications. The most important properties for electrode materials of supercapacitors are a high specific capacitance and durable CV (cyclic voltammetry) characteristics.

Electrochemical capacitors (i.e., supercapacitors) can be categorized into two types according to their charge/discharge mechanisms [1,2]. The first type is termed a electrical double-layer capacitor (EDLC). It stores energy by electrostatic adsorption/desorption between polarized solid electrode vertical line liquid electrolyte interfaces. In particular, carbon aerogel is a most promising material as an electrode for EDLCs, as it allows an interconnected three-dimensional network structure, a high specific surface-area, good electrical conductivity and a suitable pore size for common electrolytes [3,4]. The second type is a pseudocapacitor that can store energy via surface faradaic redox reactions on the interface of the electroactive material and the electrolyte. This pseudocapacitor with a large capacitance is made possible by electrode material that can be reversibly oxidized and reduced over a wide potential range. Therefore, transition metal oxides (e.g., RuO$_2$, NiO, and MnO$_2$) and conducting polymers with various oxidation states are considered as promising materials for pseudocapacitors because of the capacitance generated from the reversible redox transitions of the electroactive materials [5].

In addition to studies regarding the electrode material for each type of supercapacitor, several studies [6–12] relating to a combination of pseudocapacitive materials and carbonaceous materials suitable for EDLCs have been conducted in an effort to improve the electrochemical performance. Among the above approaches, ruthenium oxide (RuO$_2$) with its extraordinary capacitance properties has been found to have the highest potential as a pseudocapacitive material [1,6–11]. On the other hand, wide usage of ruthenium oxide in supercapacitor applications has been limited due to its rarity and high cost.

As an alternative or co-material for ruthenium oxide, tin oxide is noted for its high electrical conductivity [7] and excellent

* Corresponding author. Tel.: +82 2 2123 2850; fax: +82 2 365 5882.
E-mail address: prohsh@yonsei.ac.kr (S.-H. Hyun).

pseudocapacitive properties for use in electrochemical capacitors [5,7]. It is widely used as a catalytic material, a gas sensor, an anode material in secondary lithium batteries, and transparent conductive films for displays and solar cells [13].

The objective of this research includes developing optimum methods for synthesizing carbon aerogel-based composite electrodes for supercapacitors. In this work, tin oxide has been selected as an additive material in carbon aerogels to combine the advantage of pseudocapacitive tin oxide and carbon aerogels and to improve the overall electrochemical performance of the composite electrodes. The effect of the addition of tin oxide on the physical/electrochemical properties of composite electrodes is experimentally investigated, and the effectiveness of two different methods for synthesizing composite electrodes is elucidated.

2. Experimental procedure

The fabrication methods for resorcinol–formaldehyde (RF)/carbon aerogels used in this work have been described in detail in the previous studies by the authors [3,4]. A schematic representation of the synthesis of the tin oxide/carbon aerogel composite electrode is given in Fig. 1.

2.1. Method I: impregnation of SnO_2 sol into RF wet gels

Resorcinol–formaldehyde wet gels (solid content of 40 wt.%, resorcinol:catalyst molar ratio of 1000) were prepared via aqueous polycondensation of resorcinol in formaldehyde using sodium carbonate as a base catalyst. The synthesized RF wet gels were immersed in SnO_2 sol for 0–96 h (see Fig. 1, Method I). The SnO_2 sol was synthesized by a method similar to that presented by Siciliano [13]. The as-received sol had a very low pH (0.91) and a sub-nano scale particle size. Following the synthesizing process, the pore liquids in the RF wet gels were exchanged with acetone. Multiple exchanges with fresh acetone were performed over 4 days to remove residual water and SnO_2 sol from the pores of the RF wet gels.

Ambient drying was performed at room temperature for 3 days and at 50 °C in an oven for 1 day via the controlled evaporation of the pore liquid in an acetone atmosphere. The dimensions of the dried SnO_2-impregnated RF aerogel composite were then measured to evaluate the bulk density, porosity and shrinkage during ambient drying.

After the ambient drying procedure, pyrolysis of the SnO_2-impregnated RF aerogels was carried out under a continuous nitrogen flow in a tube furnace. Details of the pyrolysis conditions have been presented in previous work [4]. The synthesized aerogels were cut into a disc with a thickness of 1 mm, and activated at 450 °C in a hot air environment for 1 h to modify the surface functionality and improve the affinity with the electrolyte.

2.2. Method II: impregnation of ethanol-based $SnCl_4$ solution into carbon aerogels

Carbon aerogels were synthesized by the pyrolysis of RF aerogels. The carbon aerogels were then cut into disc-type elec-
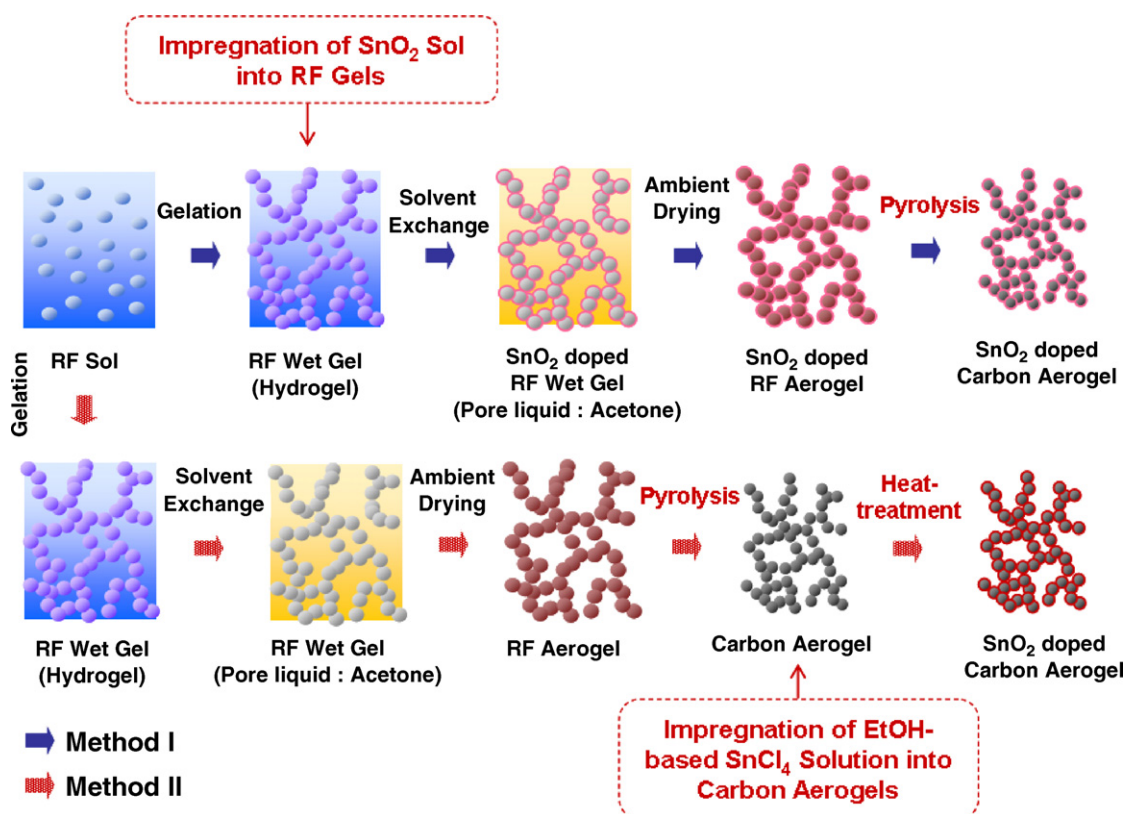

Fig. 1. Schematic representation of two different impregnation methods used in this work.

trodes with a thickness of 1 mm. After cleaning and drying, the carbon aerogel electrodes were immersed in an ethanol-based SnCl$_4$ solution for 0–60 min (see Fig. 1, Method II) and were ultrasonically treated at 28 kHz. This solution was created by vigorous mixing of reagent grade anhydrous tin tetrachloride (SnCl$_4$, Junsei pure chem., Japan) and ethanol (C$_2$H$_5$OH, Duksan pure chem., Korea) at a 0.1:1 molar ratio. After sonochemical impregnation, the tin precursor-impregnated carbon aerogel electrodes were dried at room temperature and then heat-treated at 450 °C for 1 h for activation of the carbon surface and for complete oxidation of the tin precursors.

2.3. Characterization

The specific surface-area of tin oxide-impregnated aerogels was determined by the Brunauer–Emmett–Teller (BET) method (Gemini 2375, Micromeritics Instrument Group, USA). A four-point probe method was used to measure the electrical conductivity of the electrodes at room temperature. The surface morphology, microstructures and EDX (energy dispersive X-ray) results were obtained by environmental scanning electron microscopy (ESEM, FEIXL-30 FEG, Philips, Netherlands).
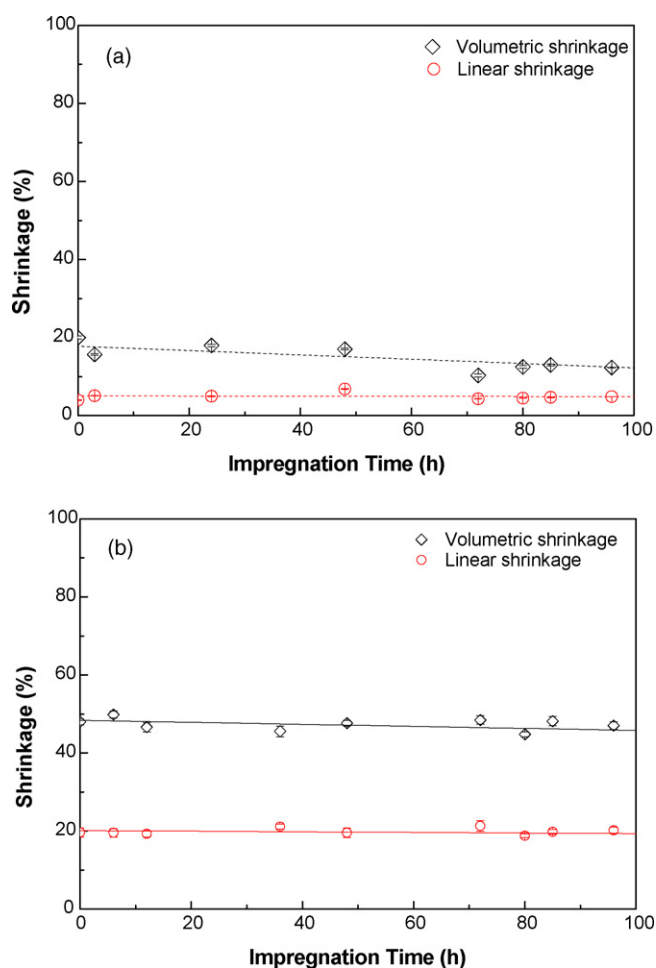
In this work, a typical galvanostatic charge/discharge method and cyclic voltammetry were used to carry out the electrochemical characterization. The structure and design of the electrochemical test cell for these measurements has been described in detail in a previous work [3]. Before any measurements were taken, the electrodes were placed in 1 M sulfuric acid electrolyte solution for 24 h to ensure complete filling of the porous electrodes. The specific capacitance of two electrodes was calculated from the charge/discharge curve using Eq. (1):

$$C = \frac{I\Delta t}{m\Delta V},$$
(1)

where C is the specific capacitance (F g^{-1}) of two electrodes (i.e., the capacitance of the full cell), I is the constant current, Δt is the time period, m is the mass of the electrodes, and ΔV is the potential differences. Cyclic voltammetry was measured between -1.0 and 1.0 V at a scan rate of 1 mV s^{-1} using a d.c. battery cycler (WBCS3000, WonATech, Korea). The potentiostatic effective capacitance of the electrodes was calculated from the cyclic voltammogram using Eq. (2):
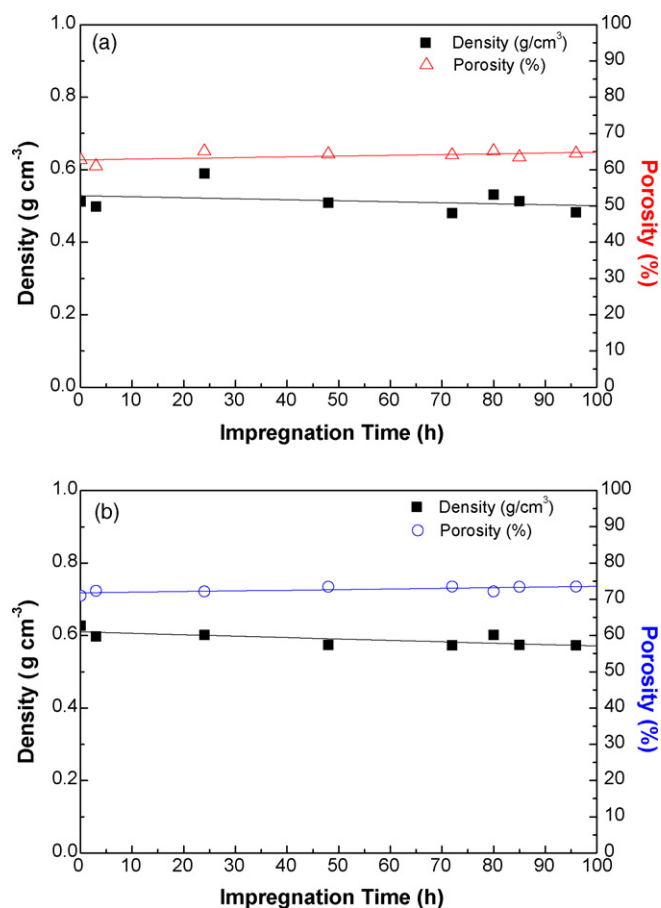
$$C = \int \frac{i}{dV/dt}$$
(2)

Fig. 2. Shrinkage behaviour of SnO$_2$-impregnated RF/carbon aerogels (synthesized by Method I) according to impregnation time during (a) ambient drying and (b) pyrolysis. An impregnation time of zero indicates values for pure RF/carbon aerogels.

Fig. 3. Bulk density and porosity variations of SnO$_2$-impregnated RF/carbon aerogels (synthesized by Method I) with impregnation time: (a) RF aerogel and (b) carbon aerogels. An impregnation time of zero indicates values for pure RF/carbon aerogels.
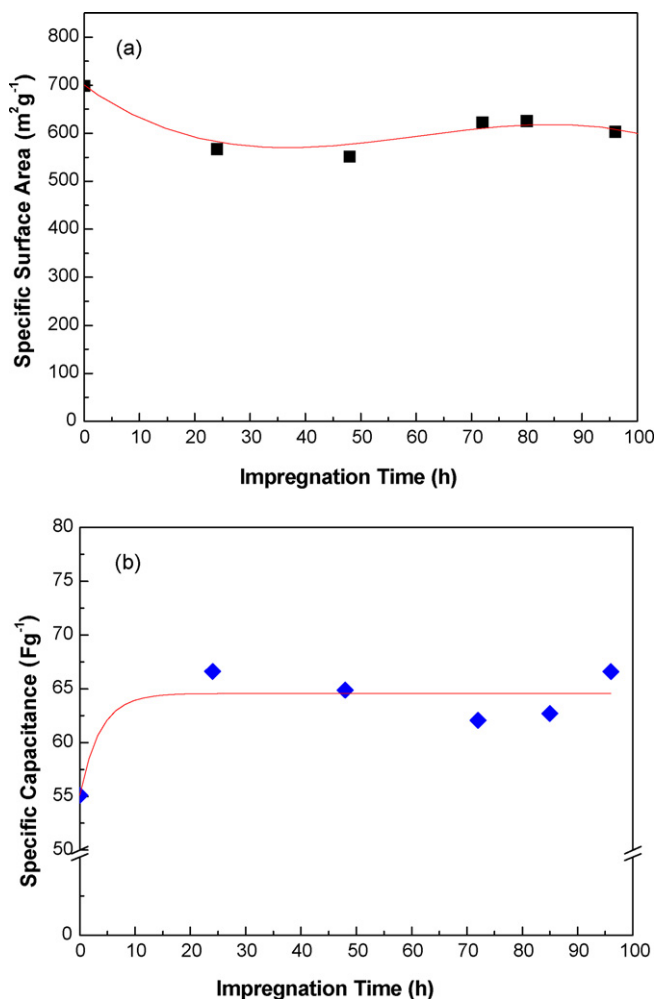
Fig. 4. Properties of SnO$_2$-impregnated carbon aerogels depending on impregnation time: (a) specific surface-area and (b) specific capacitance. An impregnation time of zero indicates values for pure-carbon aerogels.
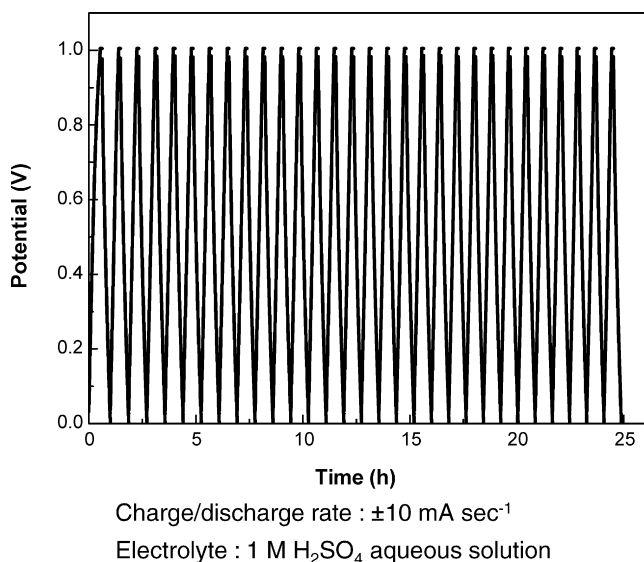

Charge/discharge rate : ±10 mA sec^{-1}

Electrolyte : 1 M H$_2$SO$_4$ aqueous solution

Fig. 5. Charge/discharge curve of SnO$_2$-impregnated carbon aerogel electrodes. Impregnation time is 24 h.

where i is the average current in the linear region of either the cathodic and anodic response and dV/dt is the scan rate.

3. Results and discussion

3.1. Tin oxide/carbon aerogel composite electrodes synthesized from SnO$_2$ sol-impregnated RF gels (by Method I)

The shrinkage behaviour during the ambient drying process of the SnO$_2$ sol-impregnated RF wet gels and pyrolysis of SnO$_2$ sol-impregnated RF aerogel is given in Fig. 2. From the graphs, the points at which the impregnation time is zero indicate the value of the pure RF and carbon aerogels. Both the linear and the volumetric shrinkage rates during the ambient drying and pyrolysis processes are independent of the SnO$_2$ sol impregnation time. In addition, these values are nearly similar to those of pure aerogels. In particular, the linear shrinkage rates during the ambient drying process are nearly constant at less than 4.5%, while the volumetric shrinkage rates decrease slightly as the impregnation time increases.

Fig. 3a and b gives the density and porosity variations of the SnO$_2$-impregnated RF and carbon aerogels, respectively,
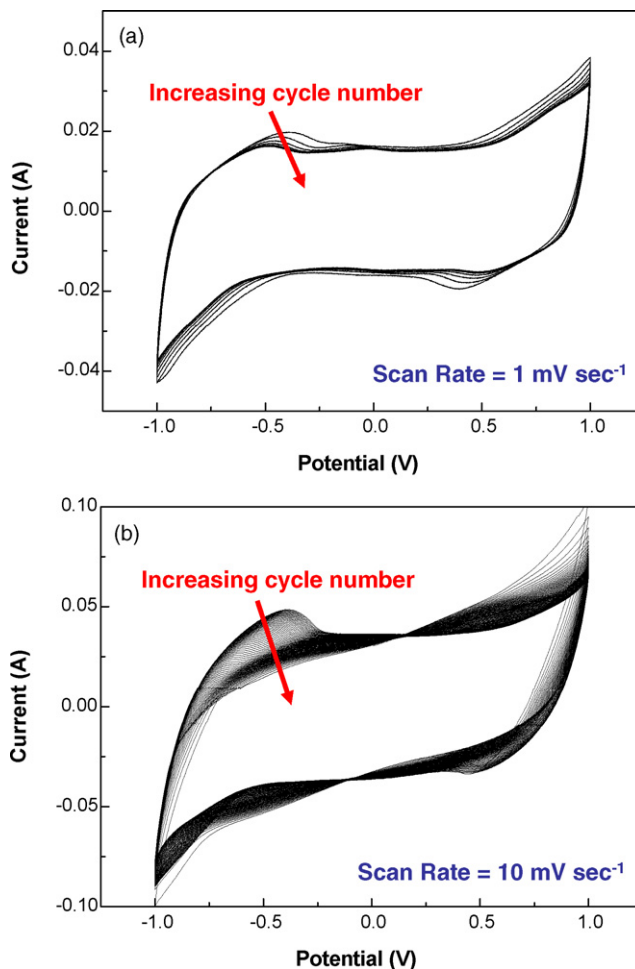

Fig. 6. Cyclic voltammograms of SnO$_2$-impregnated carbon aerogel electrodes with cycling. Sweep rate of (a) 1 mV s^{-1} (10 cycles) and (b) 10 mV s^{-1} (80 cycles).

depending on the impregnation time of the RF wet gels in SnO_2 sol. The behaviour of the bulk density and porosity versus the impregnation time is nearly identical to that of the shrinkage rates. The bulk density and porosity of SnO_2-impegnated RF aerogels are 0.47–0.53 g cm^{-3} and 60–65%, respectively. After pyrolysis in an N_2 environment, the SnO_2-impregnated carbon aerogels density slightly in the range 0.57–0.62 g cm^{-3} as the impregnation time increases, but the porosities increase to 70–73%.

The specific surface-area of the SnO_2-impregnated carbon aerogel electrodes is shown in Fig. 4a. Although the value of the pure-carbon aerogel is 700 m^2 g^{-1}, the specific surface-areas of SnO_2-impregnated electrodes have lower values than those of pure-carbon aerogel. However, the specific capacitance of the SnO_2-impregnated carbon aerogel electrodes, as calculated from the galvanostatic charge/discharge curves, increase into the range of 62.5–66.6 F g^{-1}, although the highest specific capacitance of pure-carbon aerogel is 55 F g^{-1}.

Fig. 5 show a galvanostatic charge/discharge curve for a SnO_2-impregnated carbon aerogel electrode synthesized from a RF wet gel impregnated in SnO_2 sol for 24 h. This curve has a nearly linear shape during the charging and discharging steps with charge and discharge rates of 10 and -10 mA s^{-1}, respec-

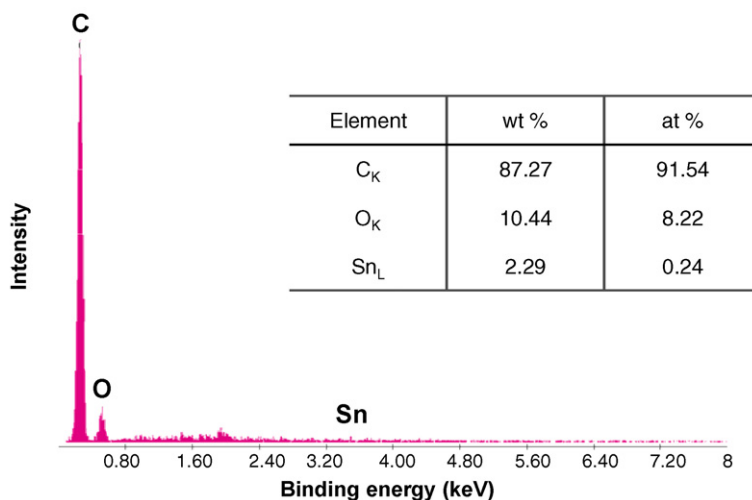tively, in an electrolyte containing 1 M sulfuric acid aqueous solution.

Cyclic voltammograms of SnO_2-impregnated carbon aerogel electrodes with increasing cycle number and different scan rates are presented in Fig. 6. As shown in Fig. 6a and b, symmetric peaks originating from the surface faradaic redox reactions are observed at scan rates of 1 and 10 mV s^{-1}. These peaks degrade gradually with cycling and this tendency becomes more pronounced at higher scan rates, as shown in Fig. 6b.

Fig. 7 presents a SEM/EDX mapping image and the EDX results of the composite electrode. The bright spots in the EDX mapping indicate the tin-containing phase attached to the network structures of carbon nanoparticles. This phase appears to be evenly dispersed on the aerogel structure. At this microscopic level, however, the amount of tin in the composite electrode is very low (2.29 wt.%), as confirmed by the EDX results.

Contrary to what was expected, the above results reveal that the impregnation of SnO_2 sol in the RF wet gel is not a viable method to enhance the electrochemical performance of tin oxide/carbon aerogel composite electrodes. Although the purpose of this approach is related to the pseudocapacity that originates from the uniformly-distributed tin oxide nanoparti-

SEM Image
Impregnation Time = 85 h
1 µm

EDX Mapping
Spots : Sn
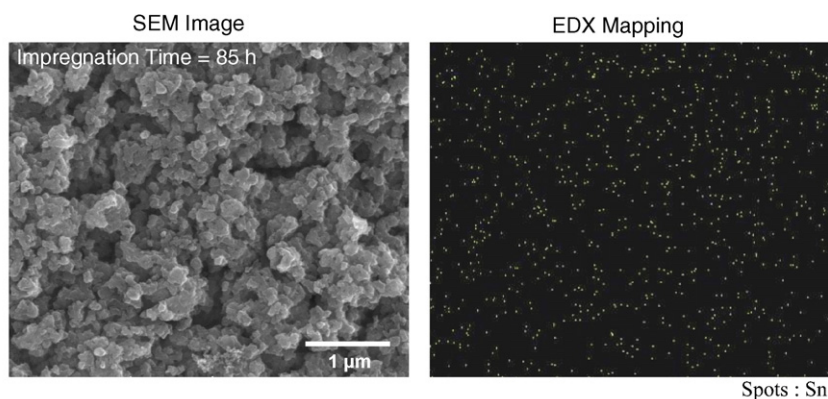
(a) SEM and EDX images of SnO_2-impregnated carbon aerogel electrodes (fractured surface).

Element	wt %	at %
C_K	87.27	91.54
O_K	10.44	8.22
Sn_L	2.29	0.24

(b) EDX result of SnO_2-impregnated carbon aerogel electrodes.

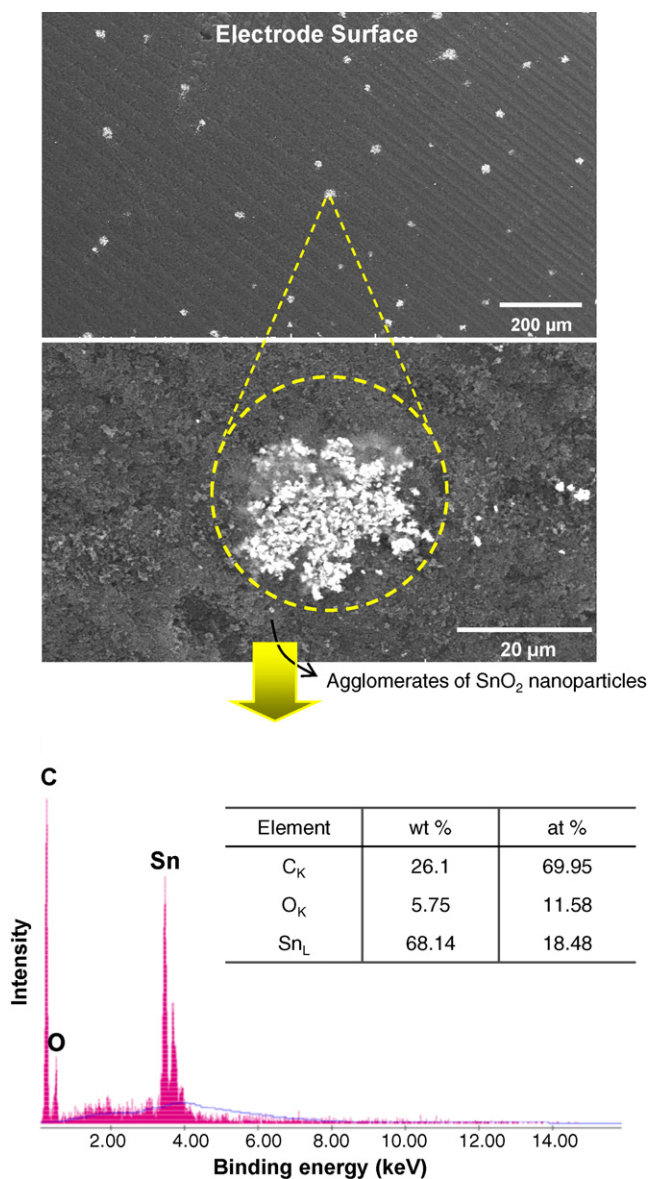Fig. 7. Microstructure and composition of SnO_2-impregnated carbon aerogel electrode.

Fig. 8. SEM images and EDX results: surface of SnO_2-impregnated carbon aerogel electrode.

Element	wt %	at %
C_K	26.1	69.95
O_K	5.75	11.58
Sn_L	68.14	18.48

cles in the mesoporous network of the aerogel matrix, as shown in Fig. 8, most of the SnO_2 particles do not penetrate the mesoporous network of the aerogel but instead aggregate in the cavities or macropores of the aerogel matrix. Thus, this non-uniformity of the tin oxide phase may give rise to the poor cyclic stability of the composite electrodes, while the specific capacitance increases slightly.

3.2. SnO2/carbon aerogel composite electrode (by Method II)

The effect of the impregnation time in the ethanol-based $SnCl_4$ solution on the specific surface-area and electrical conductivity of the composite electrodes is shown in Fig. 9. As the impregnation time increases, the specific surface-area of the composite electrode diminishes significantly while the electrical
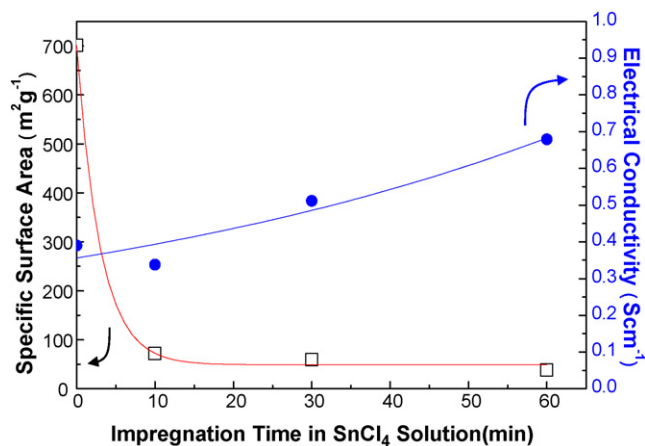

Fig. 9. Specific surface-area and electrical conductivity variations of SnO_2/carbon composite aerogels depending on impregnation time in $SnCl_4$ solution.

conductivity increases slightly. Despite the sharp decrease in the surface-area, an increase in the specific capacitance to $69.8\,F\,g^{-1}$ is observed, as demonstrated in Fig. 10. This enhancement of the specific capacitance compared with the pure-carbon aerogel is caused by the tin oxide phase, which is distributed uniformly over the network structure of the carbon aerogel. The SEM image, EDX mapping and EDX results presented in Fig. 11 are evidence of the above description. The SEM image in Fig. 11a reveals a bright phase on the carbon aerogel network. Compared with the original microstructure of carbon aerogel [4] and the EDX mapping image, this bright phase appears to be tin oxide on the carbon aerogel networks.

The effect of tin oxide in composite electrodes on the electrochemical performance is shown in the cyclic voltammogram on Fig. 12. In comparison with the former case (see Fig. 6), this composite electrode exhibits relatively good cyclic stability. Generally, ideal double-layer capacitance behaviour of a carbonaceous material is expressed in the form of a rectangular shape on the voltammetry characteristics [4]. The sign of the
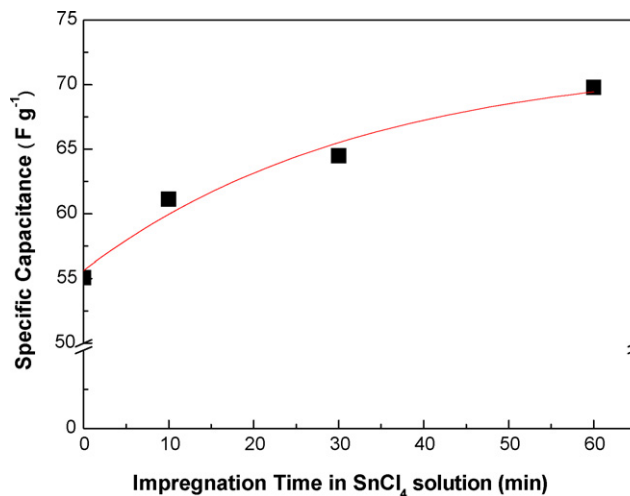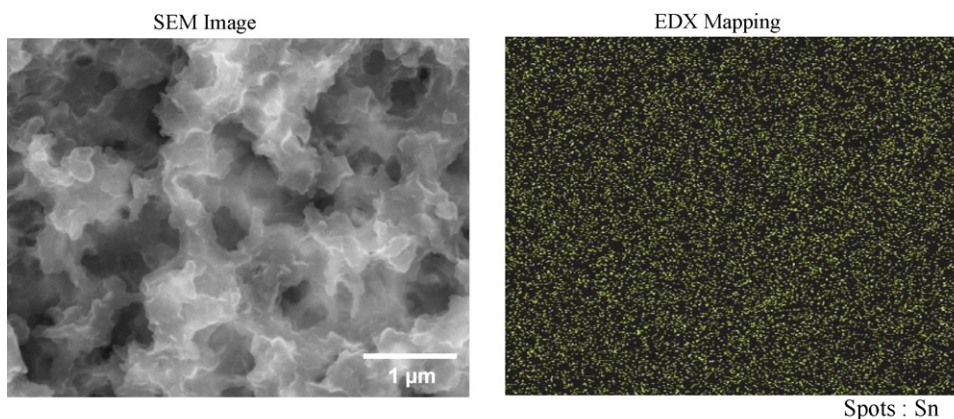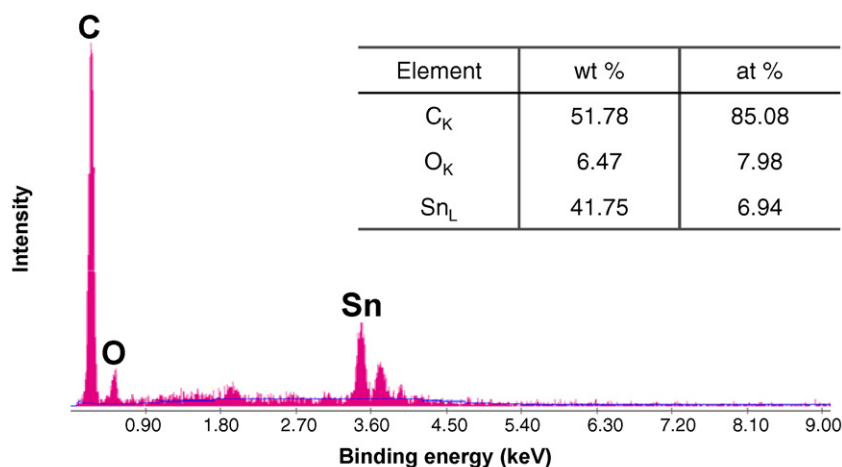

Fig. 10. Specific capacitance of SnO_2/carbon aerogel composite electrodes depending on impregnation time in $SnCl_4$ solution.

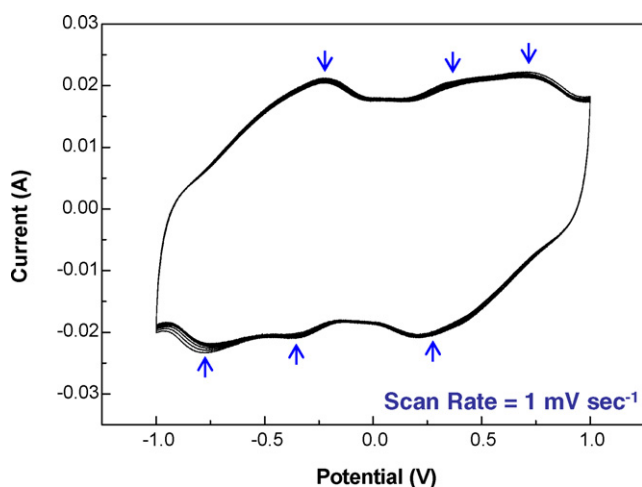(a) SEM and EDX images of SnO$_2$/carbon aerogel composite electrodes.

Element	wt %	at %
C$_K$	51.78	85.08
O$_K$	6.47	7.98
Sn$_L$	41.75	6.94

(b) EDX result of SnO$_2$/carbon aerogel composite electrodes.

Fig. 11. SEM image and EDX results of SnO$_2$/carbon aerogel composite electrodes: impregnation time in SnCl$_4$ solution is 60 min.

Impregnation for 60 min in SnCl$_4$ solution

Potentiostatic Effective Capacitance = 119.2 F g^{-1}

↓ : Influence of redox reaction

Cycling Numbers : 16 cycles

Fig. 12. Cyclic voltammogram of SnO$_2$/carbon aerogel composite electrode.

current is immediately reversed upon reversal of the potential. By contrast, an electrode material with pseudocapacitive properties gives a deviation from such a rectangular shape and the reversible redox peaks associated with the surface faradaic reactions are remarkable [1]. As seen in Fig. 12, symmetrical peaks originating from the pseudocapacitive tin oxide occur at potential windows between ±0.23, ±0.36 and ±0.76 V. These peaks arise from rapid faradaic charge-transfer reactions in addition to electrostatic charging. The proposed faradaic charge–discharge reaction in aqueous electrolyte is suggested below Eq. (3):

$$SnO_x(OH)_y + \delta H^+ + \delta e^- \Leftrightarrow SnO_{x-\delta}(OH)_{y+\delta} \tag{3}$$

From cyclic voltammetry of the composite electrode, a large current and a symmetrical type of voltammogram with a rectangular shape are found in both the anodic and cathodic directions within a wide potential window (−1.0 to 1.0 V). These features are an indication of the cathodic original capacitive nature of the tin oxide/carbon aerogel composite electrode synthesized in this work.

Therefore, the high electrochemical performance of the composite electrode can be attributed to surface faradaic redox reactions of the doped tin oxide phase in addition to the origi-
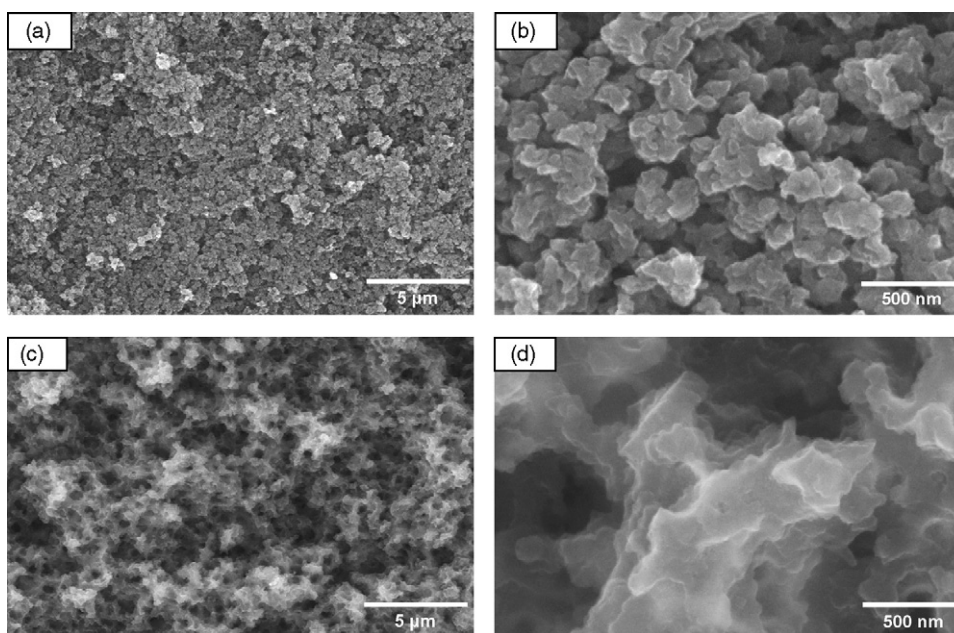
Fig. 13. SEM micrographs of SnO$_2$-impregnated carbon aerogel electrodes (fractured surface) synthesized by two different methods: (a) and (b) by Method I and (c) and (d) by Method II.

nal electrical double-layer capacitance of carbon aerogels with good cyclic stability.

The morphological and microstructural changes in the composite electrodes caused by different methods of prepared tin oxide addition are shown in Fig. 13. The composite electrode synthesized by impregnation of SnO$_2$ sol in the pores of RF wet gels (Method I) has a microstructure that is nearly identical to that of pure-carbon aerogel [4], as shown in Fig. 13a and b. By contrast, the micrographs of the composite electrodes synthesized by Method II given in Fig. 13c and d reveal quite different morphologies compared with pure-carbon aerogels. This change in morphology reveals the effective formation of the composite structure by the sono-chemical impregnation of tin precursor into the carbon aerogel electrodes. The enhancement of the electrochemical performance (i.e., an increase in specific capacitance and good cyclic stability) also corroborates the above description. Consequently, the direct sono-chemical impregnation process (Method II) can be considered as an effective method for the fabrication of tin oxide/carbon aerogel composite electrodes.

4. Conclusions

SnO$_2$/RF (resorcinol–formaldehyde) composite aerogels (specific surface-area of ∼300 m^2 g^{-1} and density of 0.5 g cm^{-3}) have been successfully synthesized via impregnation of SnO$_2$ sol into an RF wet gel structure, followed by cost-effective ambient drying of SnO$_2$-impregnated RF wet gels in place of conventional supercritical drying. The linear shrinkage of the synthesized SnO$_2$/RF composite aerogels is less than 4% and the bulk densities are ∼0.6 g cm^{-3}. SnO$_2$/carbon composite aerogel electrodes are prepared via pyrolyzing SnO$_2$-impregnated RF organic aerogels at 800 °C

in a N$_2$ atmosphere. The specific surface-area of SnO$_2$/carbon aerogels varies between 550 and 700 m^2 g^{-1} with impregnation time, while the densities (∼0.55 g cm^{-3}) and porosities (∼75%) are nearly constant. The porosity and specific surface-area of the synthesized SnO$_2$/carbon composite aerogels are as much as ∼75% and ∼650 m^2 g^{-1} after activation at 450 °C in air for 1 h. SnO$_2$/carbon aerogel composite electrodes have also been synthesized by impregnation of an ethanol-based SnCl$_4$ solution. The specific surface-area decreases markedly with increase in impregnation time, while the electrochemical capacitances are nearly identical to those pure-carbon aerogel electrodes. The highest specific capacitances of SnO$_2$/carbon aerogel composite electrodes measured according to the galvanostatic charge/discharge method and according to cyclic voltammetry are 69.8 and 119.2 F g^{-1}, respectively. These high specific capacitances are attributed to the surface faradaic redox reactions of SnO$_2$ additives, in addition to the original electrical double-layer capacitance of carbon aerogels.

Acknowledgement

References

[1] E. Frackowiak, F. Béguin, Carbon 39 (2001) 937–950.
[2] A. Burke, J Power Sources 91 (2000) 37–50.
[3] S.J. Kim, S.W. Hwang, S.H. Hyun, J. Mater. Sci. 40 (2005) 725–731.
[4] S.W. Hwang, S.H. Hyun, J. Non-Cryst. Solids 347 (2004) 238–245.

[5] K.R. Prasad, N. Miura, Electrochem. Commun. 6 (2004) 849–852.

[6] J.W. Long, K.E. Swider, C.I. Merzbacher, D.R. Rolison, Langmuir 15 (1999) 780–785.

[7] N.L. Wu, S.L. Kuo, M.H. Lee, J Power Sources 104 (2002) 62–65.

[8] H. Kim, B.N. Popov, J Power Sources 104 (2002) 52–61.

[9] J.M. Miller, B. Dunn, Langmuir 15 (1999) 799–806.

[10] J.P. Zheng, Electrochem. Solid ST 2 (1999) 359–361.

[11] H. Kim, B.N. Popov, J. Electrochem. Soc. 150 (2003) A1153–A1160.

[12] H. Liang, F. Chen, R. Li, L. Wang, Z. Deng, Electrochim. Acta 49 (2004) 3463–3467.

[13] P. Siciliano, Sens. Actuators B-Chem. 70 (2000) 153–164.